The Compact Muon Solenoid Experiment

Conference Report

Mailing address: CMS CERN, CH-1211 GENEVA 23, Switzerland

26 March 2013 (v2, 18 April 2013)

SM Higgs searches by CMS at the LHC

Mikhail Kirsanov for the CMS Collaboration

Abstract

Results are presented from searches for the standard model (SM) Higgs boson in proton-proton collisions at the CM energies of 7 and 8 TeV in five decay modes: $\gamma\gamma$, ZZ, WW, $\tau\tau$, and $b\bar{b}$. The analysed data correspond to integrated luminosities of up to 5.1 fb^{-1} at 7 TeV and up to 12.2 fb^{-1} at 8 TeV. The search is performed in the mass range 110 - 1000 GeV. No evidence is found for a significant excess of events that could be attributed to an additional particle, beyond the recently observed boson with a mass near 125 GeV. The significance of the latter is now 6.9 sigma. Its mass is measured to be $125.8 \pm 0.4(stat) \pm 0.4(syst)$ GeV. The event yields obtained by the different analyses targeting specific decay modes and production mechanisms are consistent with those expected for the SM Higgs boson . The best-fit signal strength for all channels combined, expressed in units of the SM Higgs boson cross section, is 0.88 ± 0.21. The consistency of the couplings of the observed boson with those predicted for the SM Higgs boson is tested in various ways, and no significant deviations are found. Under the assumption that the observed boson has spin zero, the data disfavour the psudo-scalar hypothesis with a CLs value of 2.4%.

Presented at *LHC on the March LHC on the March*

SM Higgs searches by CMS at the LHC

M. Kirsanov[a*],
^a *INR RAS*
Moscow

Abstract

Results are presented from searches for the standard model (SM) Higgs boson in proton-proton collisions at $\sqrt{s} = 7$ and 8 TeV in five decay modes: $\gamma\gamma$, bb, $\tau\tau$, WW, and ZZ. The analysed data correspond to integrated luminosities of up to 5.1 fb^{-1} at 7 TeV and up to 12.2 fb^{-1} at 8 TeV. The search is performed in the mass range 110 - 1000 GeV. No evidence is found for a significant excess of events that could be attributed to an additional particle, beyond the recently observed boson with a mass near 125 GeV. The significance of the latter is now 6.9 σ. Its mass is measured to be $125.8 \pm 0.4(stat) \pm 0.4(syst)$ The event yields obtained by the different analyses targeting specific decay modes and production mechanisms are consistent with those expected for the SM Higgs boson. The best-fit signal strength for all channels combined, expressed in units of the SM Higgs boson cross section, is 0.88 ± 0.21. The consistency of the couplings of the observed boson with those predicted for the SM Higgs boson is tested in various ways, and no significant deviations are found. Under the assumption that the observed boson has spin zero, the data disfavour the psudo-scalar hypothesis with a CL_s value of 2.4%.

1 Introduction

The Standard Model (SM) [1], [2] of particle physics has been very successful in explaining experimental data. In the SM the Higgs mechanism is postulated in order to explain the origin of the masses of the W and Z bosons that arise from electroweak symmetry breaking, which leads to an additional scalar field whose quantum, the Higgs boson, should be experimentally observable [3], [4].

The mass of the Higgs boson is not fixed in the Standard Model. The constraints on it are derived from the following considerations [5]:

- "Unitarity": Higgs boson exchange allows to avoid unphysical W - W scattering probability at high energies if $M_H < 800$ GeV

- "Triviality": Higgs boson self-coupling becomes too strong (so that perturbative methods are not applicable) if its mass is higher than some value depending on the cut-off scale Λ. This value has significant uncertainties, approximately it is given by $M_H^2 < 4\pi^2\nu^2/(3ln(\Lambda/\nu))$.

- "Stability" of the vacuum: potential $V(\phi)$ has only one absolute minimum. Requires $M_H^2 > m_t^4 ln(\Lambda/\nu)/\pi^2\nu^2$

Here ν is the vacuum-expectation value of the Higgs field and Λ is the cut-off scale.

In various extentions of the SM the Higgs sector can be more complicated, with additional observable particles.

---

*e-mail: Mikhail.Kirsanov@cern.ch

The LHC and its major experiments were conceived and built to explore in depth the multi-TeV region and solve in a way or in another this major puzzle of particle physics. Excellent performance of the LHC in 2011 and 2012 allowed to the experiments to collect enough data to reach sensitivity exceeding or close to the SM Higgs boson cross sections. The teams of physicists of the ATLAS and CMS experiments managed to quickly perform the analysis of data in complicated conditions of pile-up (multiple proton-proton interactions in one bunch crossing, 10 - 15 on the average) and high backgrounds (cross sections up to 10^{11} of the Higgs boson cross sections). As a result of this work a boson with a mass of about 125 GeV with properties compatible with the SM predictions for the Higgs boson was recently observed [6] [7].

The results of the continuation of the searches for particles similar to the SM Higgs boson in the CMS experiment and further studies of the previously observed boson are presented in this paper.

2   The CMS detector

A detailed description of the CMS detector can be found elsewhere [8]. The main features and those most pertinent to this analysis are described below. The central feature is a superconducting solenoid, 13 m in length and 6 m in diameter, which provides an axial magnetic field of 3.8 T. The bore of the solenoid is instrumented with particle detection systems. The steel return yoke outside the solenoid is instrumented with gas detectors used to identify muons. Charged particle trajectories are measured by the silicon pixel and strip tracker, with full azimuthal coverage within $|\eta| <$2.5, where the pseudorapidity η is defined as $\eta = -ln[tan(\Theta/2)]$, with Θ being the polar angle of the trajectory of the particle with respect to the counterclockwise beam direction. A lead-tungstate crystal electromagnetic calorimeter (ECAL) and a brass/scintillator hadron calorimeter (HCAL) surround the tracking volume and cover the region $|\eta| <$3. The ECAL barrel extends to $|\eta| =$1.48. A lead/silicon-strip preshower detector is located in front of the ECAL endcap. A steel/quartz-fibre Cherenkov forward calorimeter extends the calorimetric coverage to $|\eta| <$5.0. In the region $|\eta| <$1.74, the HCAL cells have widths of 0.087 in both pseudorapidity and azimuth (ϕ). In the (η, ϕ) plane, and for $|\eta| <$1.48, the HCAL cells map on to 5x5 ECAL crystal arrays to form calorimeter towers projecting radially outwards from points slightly offset from the nominal interaction point. In the endcap, the ECAL arrays matching the HCAL cells contain fewer crystals. Calibration of the ECAL uses π^0s, $W \rightarrow e\nu$, and $Z \rightarrow ee$. Deterioration of transparency of the ECAL crystals due to irradiation during the LHC running periods and their subsequent recovery is monitored continuously and corrected for using light injected from a laser and LED system.

3   SM Higgs boson production and decays

There are four main mechanisms for Higgs boson production in pp collisions. The gluon-gluon fusion mechanism has the largest cross section, followed in turn by vector boson fusion (VBF), associated WH and ZH production, and production in association with top quarks, $t\bar{t}H$. The Higgs boson decay modes are determined by its nature, in particular by the fact that its coupling to elementary particles (except gauge bosons, for which the dependency is more complicated) is proportional to their masses. This means that it prefers to decay to heavy particles. For the same reason the brancing ratios depend strongly on the Higgs boson mass m_H, as shown in Figure 1. These peculiarities of the Higgs boson decays and comparably small production cross sections render its searches rather complicated, in particular for some ranges of m_H, for example below 120 GeV. The strategy of the searches for the Higgs boson are in turn determined by the peculiarities mentioned above. The decays modes most relevant to the searches at the LHC are listed in Table 1.

Table 1: Summary of the SM Higgs boson decay channels and production modes relevant for the searches and studies at the LHC

Channel	Masses [GeV]	Branch. ratio	N_{ev}, 10 fb^{-1}	Prod. modes	S/B	Mass res.	Remark
$H \to \gamma\gamma$	110 - 150	2×10^{-3}	200/400	inclusive, VBF	low O(0.1)	2%	max. sens. at low mass
$H \to bb$	110 - 135	0.7	$30/10^5$	VH	low O(0.1)	10%	
$H \to \tau\tau$	110 - 150	0.08	$20/10^4$	inclusive, VBF, VH	low O(0.1)	15%	
$H \to WW^{(*)} \to l\nu l\nu$	110 - 700	0.03	$60/10^3$	gg fusion, VBF, VH	medium O(1)	-	max. sens. at interm.
$H \to ZZ^{(*)} \to 4l$	110 - 700	$(3\text{–}8) \times 10^{-4}$	6/20	inclusive	high >1	2%	
$H \to ZZ \to other$	200 - 700	0.2	-	inclusive		10%	max. sens. at high mass
$H \to WW \to l\nu qq$	170 - 700	0.15	-	inclusive			

Table 2: Summary of Higgs analyses and documentation

Channel	Masses [GeV]	Data used, fb^{-1} (7 + 8 TeV)	References	Remarks
$H \to \gamma\gamma$	110 - 150	5.1 + 5.3	HIG-12-15	Mass measurement
$H \to bb$	110 - 135	5 + 12.1	HIG-12-44	
$H \to \tau\tau$	110 - 145	4.9 + 12.1	HIG-12-43	
$H \to WW^{(*)} \to l\nu l\nu$	110 - 700	4.9 + 12.1	HIG-12-42	
$H \to ZZ^{(*)} \to 4l$	110 - 700	5.1 + 12.2	HIG-12-41	Mass and parity measurements
Higgs combination	110 - 700	4.9–5.1 + 5.3–12.2	HIG-12-45	
$H \to WW \to l\nu qq$	170 - 700	5 + 12	HIG-12-46	

There are three types of independent theoretical uncertainties on Higgs boson production: uncertainties associated with (i) parton density functions (PDFs), (ii) incomplete perturbative calculations (also known as QCD scale uncertainties), and (iii) the treatment of the finite width of the Higgs boson. All these uncertainties are taken from Ref. [9].

4 Higgs boson searches in the CMS detector

The CMS analyses and references to the corresponding public documentation are shown in Table 2.

The $WW^{(*)} \to 2l2\nu$ analysis [10] searches for an excess of events with two leptons of opposite charge, large E_T^{miss}, and up to two jets. Events are divided into six categories, with different background compositions and signal-to-background ratios. For events with no jets, the main background stems from non-resonant WW production; for events with one jet, the dominant backgrounds are from WW and top-quark production. The events are split into same-flavour and different-flavour dilepton sub-channels, since the background from Drell- Yan production is much larger for the same-flavour dilepton events. The two-jet category is optimized to take advantage of the VBF Higgs boson production signature. The main back ground in this channel is from top-quark production. In the 7 TeV analysis, the same-flavour and different-flavour categories with 2 jets are merged into one. To improve the separation of signal from

3

backgrounds in the 7 TeV analysis, MVA classifiers are trained for a number of Higgs boson masses. The search is made for an excess of events in the output distributions of the classifiers. Similarly, in the 8 TeV analysis the bidimensional distribution of events in the (m_{ll}, m_T) plane is used for different-flavour dilepton channels with zero and one jet; m_{ll} is the invariant mass of the dilepton pair, and m_T is the transverse mass reconstructed from the transverse momentum of the dilepton and the missing transverse momentum. Using the bidimensional distributions allowed to improve significantly the sensitivity of the analysis as compared to the previous one made with 5 fb^{-1} of 8 TeV data. All background rates, except for very small contributions from WZ, ZZ, and Wγ, are evaluated from data.

In the $H \to ZZ \to 2\ell2\tau$ search [11], one Z boson is required to be on-shell and to decay to a lepton pair (ee or $\mu\mu$). The other Z boson is required to decay through a $\tau\tau$ pair to one of the four final-state signatures $e\mu$, $e\tau_h$, $\mu\tau_h$, $\tau_h\tau_h$. Thus, eight exclusive sub-channels are defined. We search for a broad excess in the distribution of the dilepton-ditau mass, constructed from the visible products of the tau decays, neglecting the effect of the accompanying neutrinos. The dominant background is non-resonant ZZ production whose rate is estimated from simulation. The main sub-leading backgrounds with jets misidentified as τ leptons stem from $Z + \text{jets}$ (including ZW) and top-quark events. These backgrounds are estimated from data.

In the $H \to ZZ^{(*)} \to 4\ell$ channel [11], we search for a four-lepton mass peak over a small continuum background. This is extremely clean, high resolution channel, often called "Golden", but with a very low rate. For this reason high trigger and selection efficiencies are very important. Collision events are selected by the trigger system that requires the presence of a pair of electrons or a pair of muons, or a triplet of electrons. A trigger requiring an electron and a muon is also used for the 2012 data. The trigger efficiency is higher than 98%. To further separate signal and background, a matrix element likelihood analysis (MELA) is used. Five angles $\Theta^*, \Phi_1, \Theta_1, \Theta_2, \Phi$ defined in [12], and the invariant masses of the lepton pairs, m_{Z_1} and m_{Z_2}, fully describe the kinematics of the $H \to ZZ \to 4l$ process at a given mass of the four-lepton system in their centre-of-mass frame. These observables provide significant discriminating power between signal and background. We construct a kinematic discriminant (K_D) based on the probability ratio of the signal and background hypotheses, MELA $K_D = P_{sig}/(P_{sig} + P_{bkg})$, as described in [12], [13]. The likelihood ratio is defined for each value of m_{4l}. The 4e, 4μ, 2e2μ sub-channels are analyzed separately since there are differences in the four-lepton mass resolutions and the background rates arising from jets misidentified as leptons. The dominant irreducible background in this channel is from non-resonant ZZ production (with both Z bosons decaying to either 2e, or 2μ, or 2τ with the taus decaying leptonically) and is estimated from simulation. The smaller reducible backgrounds with jets misidentified as leptons, e.g. $Z + \text{jets}$, are estimated from data. This analysis (including $2\ell2\tau$) excludes the SM Higgs boson at 95% CL. in the ranges $113 < m_H < 116$ GeV, $129 < m_H < 720$ GeV. The local significance of the excess at 125.5 is 4.4 σ (expected for the SM Higgs 5 σ). The best fit signal strength at 125 GeV is 0.74 ± 0.25. The mass fit gives 126.2 ± 0.6 (stat) ± 0.2 (syst) GeV.

The statistics used in the analysis $H \to ZZ^{(*)} \to 4\ell$, significantly increased w.r.t. the previous result [6], allowed to perform for the first time the parity measurement of the discovered boson. Here we follow the MELA methodology, where instead of signal-to-background probability ratio we construct probability ratio for two signal hypotheses. The data disfavors the pseudoscalar hypothesis 0^- with a CL_s value of 2.4%.

The $H \to \gamma\gamma$ analysis [6], [14] is focused on a search for a narrow peak in the diphoton mass distribution. This is the most important channel in the low mass range. The event sample is split into two mutually exclusive classes: (i) diphoton events with one forward and one backward jet, consistent with the VBF topology, and (ii) all remaining events. This division is motivated by the consideration that there is a better signal-to-background ratio in the first class than in the second. For the 8 TeV data, the dijet class is split into two sub-classes: events with low and high dijet mass m_{jj}. The non-dijet class, containing over 99% of the data, is

subdivided into four sub-classes based on the output of a multivariate discriminant that assigns a high score to signal-like events, based on (i) an event-by-event estimate of the diphoton mass resolution, (ii) a photon identification score for each photon, and (iii) kinematic information about the photons and the diphoton system. The photon identification score is obtained from a multivariate analysis (MVA) discriminant that uses shower shape information and isolation variables to separate prompt photons from those arising from jets. The background in the signal region is estimated from a fit to the observed diphoton mass distribution in data. This analysis alone observes the excess of events above the expected standard model background for a Higgs boson mass hypothesis of 125 GeV with a local significance of 4.1 σ (expected from the SM Higgs boson 2.6 σ). The best fit signal strength at 125 GeV is 1.56 ± 0.43.

The $H \to \tau\tau$ search [15] is performed using the final-state signatures $e\mu$, $\mu\mu$, $e\tau_{\rm h}$, and $\mu\tau_{\rm h}$, where electrons and muons arise from leptonic τ-decays $\tau \to \ell\nu_\ell\nu_\tau$ and $\tau_{\rm h}$ denotes hadronic τ-decays $\tau \to {\rm hadrons} + \nu_\tau$. Each of these categories is further divided into three exclusive sub-categories based on the number and the type of the jets in the event: (i) events with one forward and one backward jet, consistent with the VBF topology, (ii) events with at least one high p_T hadronic jet but not selected in the previous category, and (iii) events with one jet with a small p_T. The last two categories are further divided by the transverse momentum of the visible tau decay. In each of these categories, we search for a broad excess in the reconstructed $\tau\tau$ mass distribution. The main irreducible background, $Z \to \tau\tau$ production, and the largest reducible backgrounds (W+ jets, multijet production, $Z \to ee$) are evaluated from various control samples in data. The treatment of the VBF category has been changed with respect to Ref. [6]. The observed upper limit on the higgs production at 125 GeV is 1.63 of the Standard Model prediction while the expected limit is on the level of the Standard Model prediction.

The search for $H \to \tau\tau$ decays produced in association with a W or Z boson is conducted in events with three or four leptons in the final state [16] The WH analysis selects events which have same charged electrons or muons and a hadronically-decaying tau: $e^+e^+\tau_{\rm h}^-$ and $\mu^+\mu^+\tau_{\rm h}^-$. The ZH analysis is performed in events with an identified $Z \to ee$ or $Z \to \mu\mu$ decay and a Higgs boson candidate with one of the following final states: $e\mu$, $e\tau_{\rm h}$, $\mu\tau_{\rm h}$, $\tau_{\rm h}\tau_{\rm h}$. The main irreducible backgrounds to the WH and ZH searches are WZ and ZZ diboson events, respectively. The irreducible backgrounds are estimated using simulation, corrected by control samples in data. The reducible backgrounds in both analyses are W, Z, and $t\bar{t}$ events with at least one quark or gluon jet misidentified as an isolated e, μ, or $\tau_{\rm h}$. These backgrounds are estimated solely from data by measuring the probability for jets to be misidentified as isolated leptons in background-enriched control regions, and weighting the selected events which fail the lepton requirements by the misidentification probability.

The $H \to bb$ search [17] concentrates on Higgs boson production in association with W or Z bosons, in which the focus is on the following decay modes: $W \to e\nu/\mu\nu$ and $Z \to ee/\mu\mu/\nu\nu$. The $Z \to \nu\nu$ decay is identified by requiring a large missing transverse energy E_T^{miss} computed from the vector sum of the transverse momenta of all reconstructed objects in the detector (leptons, photons, and charged/neutral hadrons) which are not found to arise from additional interactions. The Higgs boson candidate is reconstructed by requiring two b-tagged jets [18]. The search is divided into events where the vector bosons have medium or large transverse momentum and recoil away from the candidate Higgs boson. A multivariate regression algorithm to better estimate the b-jet p_T is trained on jets in simulated signal events and achieves a final dijet mass resolution of 8-9% for $m_H = 125$ GeV. The performance of the regression algorithm is checked in data using W, Z+jets and $t\bar{t}$ events. Events with higher transverse momentum bosons have smaller backgrounds and a better dijet mass resolution. In the 8 TeV analysis, for all final states except $Z \to ll$, the large transverse momentum events are further divided depending on whether they satisfy tight or loose b-tagging requirements. A multivariate analysis technique, trained on simulated signal and background events for several different values of the Higgs boson mass, is used to separate signal and background events. The rates of the main

backgrounds, consisting of W/Z + jets and top-quark events, are derived from signal-depleted control samples in data. The WZ and ZZ backgrounds with a Z boson decaying to a pair of b-quarks, as well as the single-top background, are estimated from simulation. The MVA output distribution is used as the final discriminant in the limit setting. This analysis observes the 2.2 σ excess of events over the background, consistent with the SM Higgs boson expectation.

5 Combination methodology

The combination of the SM Higgs boson searches requires simultaneous analysis of the data from all individual search channels, accounting for all statistical and systematic uncertainties and their correlations. The results presented here are based on a combination of Higgs boson searches in the exclusive sub-channels described in Section 4. Depending on the sub-channel, the input to the combination may be a total number of selected events or an event distribution for the final discriminating variable. Either binned or unbinned distributions are used, depending upon the particular search sub-channel.

The number of sources of systematic uncertainties considered in the combination depends on the Higgs boson mass, exceeding 200 for some masses. A large fraction of these uncertainties are correlated across different channels and between signal and backgrounds within a given channel. Uncertainties considered include: theoretical uncertainties on the expected cross sections and acceptances for signal and background processes, experimental uncertainties arising from modelling of the detector response (event reconstruction and selection efficiencies, energy scale and resolution), and statistical uncertainties associated with either ancillary measurements of backgrounds in control regions or selection efficiencies obtained using simulated events. Systematic uncertainties can affect either the shape of distributions, or event yields, or both.

The combination is repeated for more than 200 Higgs boson mass hypotheses in the range 110–1000 GeV. The step size in this scan varies across the mass range and is determined by the Higgs boson mass resolution. The minimum step size is 0.5 GeV at lower masses, where it is commensurate with the mass resolution of the $\gamma\gamma$ and $4l$ channels. The maximum step size is tens of GeV at large masses, where the intrinsic Higgs boson width is the limiting factor.

The overall statistical methodology used in this combination was developed by the CMS and ATLAS collaborations in the context of the LHC Higgs Combination Group. The detailed description of the methodology can be found in [19], [20]. Results presented in this note are obtained using asymptotic formulae [21], including a few updates recently introduced in the RooStats package [22].

The combination procedure introduces a signal strength modifier μ that multiplies the expected SM Higgs boson cross section such that $\sigma = \mu \cdot \sigma_{\mathrm{SM}}$. Each independent source of systematic uncertainty is assigned a nuisance parameter θ_i. The expected Higgs boson and background yields are functions of these nuisance parameters, and are written as $\mu \cdot s(\theta)$ and $b(\theta)$, respectively. Most nuisance parameters are constrained by other measurements. They are encoded in the probability density functions $p_i(\tilde{\theta}_i|\theta_i)$ describing the probability to measure a value $\tilde{\theta}_i$ of the i-th nuisance parameter, given its true value θ_i.

For the calculation of the exclusion limit, we adopt the modified frequentist construction CL_s [23].

$$CL_s = \frac{\mathrm{CL_{s+b}}}{\mathrm{CL_b}}. \tag{1}$$

If $CL_s \leq \alpha$ for $\mu = 1$, we determine that the SM Higgs boson is excluded at the $1 - \alpha$ confidence level. To quote the upper limit on μ at the 95% confidence level, we adjust μ until we reach $CL_s = 0.05$.

6   Results

Combined results of searches for SM Higgs bosons are presented in this section. Unless stated otherwise, the following conventions are used. The observed values are shown by a solid line. A dashed line indicates the median of the expected results for the background-only hypothesis. The green (dark) and yellow (light) bands indicate the ranges in which the measured values are expected to reside in at least 68% and 95% of all experiments under the background-only hypothesis. The probabilities for an observation to lie above or below the 68% (95%) band are at most 16% (2.5%) each. The observed and median expected values of CL_s as well as the 68% and 95% bands are obtained by generating ensembles of pseudo-datasets.

The mass regions where the observed CL_s values are smaller than 0.05 are excluded at 95% CL, the regions where they are smaller than 0.01 are excluded at 99% CL. The median expected exclusion range of m_H at 95% CL in the absence of a signal is 110–650 GeV. For the largest values of m_H, we observe fewer events than the median expected number for the background-only hypothesis, which makes the observed limits in that range stronger than expected. At small m_H we observe an excess of events due to the recently discovered new boson. This makes the observed limits weaker than expected in the absence of a SM Higgs boson. We exclude a SM Higgs boson at 95% CL in the mass range 127.5 – 700 GeV.

Figure 2 shows the 95% CL upper limits on the signal strength modifier, $\mu = \sigma/\sigma_{\mathrm{SM}}$, obtained by generating ensembles of pseudo-datasets, as a function of m_H. The ordinate thus shows the Higgs boson cross section that is excluded at 95% CL, expressed as a multiple of the SM Higgs boson cross section.

To quantify the inconsistency of the observed excesses with the background-only hypothesis, we show in Fig. 3 (left) a scan of the combined local p-value p_0 in the low-mass region. The local p-values shown in Fig. 3 are obtained with the asymptotic formula. They reach the values corresponding to 6.9 σ.

The p-value characterises the probability of background producing an observed excess of events, but it does not give information about the compatibility of an excess with an expected signal. The latter is provided by the best fit $\hat{\mu}$ value, shown in Fig. 3 (right).

7   Mass measurements

To measure the mass of the observed state, we use the $ZZ \to 4l$ and $\gamma\gamma$ channels that have excellent mass resolution and for which we observe excesses with significances of 4.4 σ and 4.0 σ, respectively. Fig. 4 (left) shows 2D 68% confidence level regions for the two parameters of interest, the signal strength modifier m and the mass mX, for these channels. The combined 68% CL contour shown with a black line in Fig. 4 (left) fixes the relative event yield between the two channels to the SM Higgs boson expectation, while the overall signal strength is left as a free parameter.

To extract the value of m_X in a model-independent way, the signal strength modifiers for the $gg \to H \to \gamma\gamma$, $VBF + VH \to \gamma\gamma$, and $H \to ZZ \to 4l$ processes are assumed to be independent and, thus, not tied to the SM expectation. The signal in all channels is assumed to be due to a state with a unique mass m_X. The mass m_X and its uncertainty are extracted from a scan of the combined test statistic $q(m_X)$ with the three signal signal strength modifiers profiled in the same way as all other nuisance parameters. Fig. 4 (right) shows the scan of the test statistic as a function of the hypothesised mass m_X for the two final states separately and their combination. Crossings of the $q(m_X)$ curves with horizontal thick (thin) lines at 1 (3.8) define the 68% (95%) CL intervals for the mass of the observed particle. These intervals include both statistical and systematic uncertainties. The 68% CL interval is $m_X = 125.8 \pm 0.5$ GeV.

To evaluate the statistical component of the overall error, we also perform a scan of the test statistic $q(mX)$ with all nuisance parameters fixed to their best-fit values. The resulting

68% CL interval is: $m_X = 125.8 \pm 0.4$ (stat) GeV. Assuming that the total error is the sum in quadrature of the statistical and systematic components, we extract a systematic error of 0.4 GeV. Therefore, the final mass measurement can be written as $m_X = 125.8 \pm 0.4$ (stat) ± 0.4 (syst) GeV.

8   Conclusions

Results are presented from searches for the standard model (SM) Higgs boson in proton proton collisions at $\sqrt{s} = 7$ and 8 TeV, using data samples corresponding to integrated luminosities of up to 5.1 fb^{-1} at 7 TeV and up to 12.2 fb^{-1} at 8 TeV. The search is performed in the mass range 110-1000 GeV in five decay modes: $\gamma\gamma$, ZZ, WW, $\tau\tau$, and bb. No evidence is found for a significant excess of events that could be attributed to an additional particle, beyond the recently observed boson with a mass near 125 GeV. The significance of the latter is now 6.9 σ. Its mass is measured to be 125.8 ± 0.4 (stat) ± 0.4 (syst) GeV. The event yields obtained by the different analyses targeting specific decay modes and production mechanisms are consistent with those expected for the SM Higgs boson. The best-fit signal strength for all channels combined, expressed in units of the SM Higgs boson cross section, is 0.88 ± 0.21. The consistency of the couplings of the observed boson with those predicted for the SM Higgs boson is tested in various ways, and no significant deviations are found. Under the assumption that the observed boson has spin zero, the data disfavour the psudo-scalar hypothesis 0^- with a CL_s value of 2.4%.

References

[1] S. L. Glashow, "Partial-symmetries of weak interactions" *Nucl. Phys.* **22** (1961) 579.

[2] S. Weinberg, "A model of leptons" *Phys. Rev. Lett.* **19** (1967) 1264.

[3] P. W. Higgs, "Broken symmetries, massless particles and gauge fields" *Phys. Lett.* **12** (1964) 132.

[4] P. W. Higgs, "Broken symmetries and the masses of gauge bosons" *Phys. Rev. Lett.* **13** (1964) 508.

[5] K. Riesselman, hep-ph/9711456.

[6] CMS Collaboration, "Observation of a new boson at a mass of 125 GeV with the CMS experiment at the LHC", *Phys. Lett. B* (2012), arXiv:1207.7235.

[7] ATLAS Collaboration, "Observation of a new particle in the search for the Standard Model Higgs boson with the ATLAS detector at the LHC", *Phys. Lett. B* (2012), arXiv:1207.7214.

[8] CMS Collaboration, "The CMS experiment at the CERN LHC" *JINST* **3** (2008) S08004.

[9] LHC Higgs Cross SectionWorking Group Collaboration, "Handbook of LHC Higgs Cross Sections: 1. Inclusive Observables", CERN CERN-2011-002, (2011).

[10] CMS Collaboration, "Evidence for a particle decaying to W+W- in the fully leptonic final state in a standard model Higgs boson search in pp collisions at the LHC", CMS Physics Analysis Summary CMS-PAS-HIG-12-042 (2012). Previous published 7 TeV result is in arXiv:1202.1489.

[11] CMS Collaboration, "Updated results on the new boson discovered in the search for the standard model Higgs boson in the ZZ to 4 leptons channel in pp collisions at sqrt(s) = 7 and 8 TeV", CMS-PAS-HIG-12-041 (2012), CERN preprint: CERN-PH-EP-2012-372

[12] Y. Gao et al., "Spin determination of single-produced resonances at hadron colliders", *Phys. Rev. D* **81** (2010) 075022, arXiv:1001.3396.

[13] S. Bolognesi, Y. Gao, A. V. Gritsan et al., "On the spin and parity of a single-produced resonance at the LHC", arXiv:1208.4018.

[14] CMS Collaboration, "Search for a standard model Higgs boson decaying into two photons in pp collisions", CMS-PAS-HIG-12-015 (2012)

[15] CMS Collaboration, "Search for standard model Higgs bosons decaying to tau pairs", CMS-PAS-HIG-12-043 (2012).

[16] CMS Collaboration, "Search for a Standard Model Higgs bosons decaying to tau pairs produced in association with a W or a Z boson", CMS-PAS-HIG-12-051 (2012).

[17] CMS Collaboration, "Search for standard model Higgs bosons produced in association with W or Z bosons, and decayng to bottom quarks" CMS-PAS-HIG-12-044 (2012).

[18] CMS Collaboration, "Algorithms for b jet identification in CMS", CMS Physics Analysis Summary CMS-PAS-BTV-09-001 (2009).

[19] ATLAS and CMS Collaborations, LHC Higgs Combination Group, "Procedure for the LHC Higgs boson search combination in Summer 2011", ATL-PHYS-PUB/CMS NOTE 2011-11, 2011/005, (2011).

[20] CMS Collaboration, "Combined results of searches for the standard model Higgs boson in pp collisions at $sqrts = 7$ TeV", *Phys. Lett. B* **13** (2012) 26.

[21] G. Cowan et al., "Asymptotic formulae for likelihood-based tests of new physics", Eur. Phys. J. C 71 (2011) 1-19, arXiv:1007.1727.

[22] L. Moneta, K. Belasco, K. S. Cranmer et al., "The RooStats Project", arXiv:1009.1003.

[23] A. L. Read, "Presentation of search results: the CLs technique", J. Phys. G: Nucl. Part. Phys. **28** (2002) 2693.
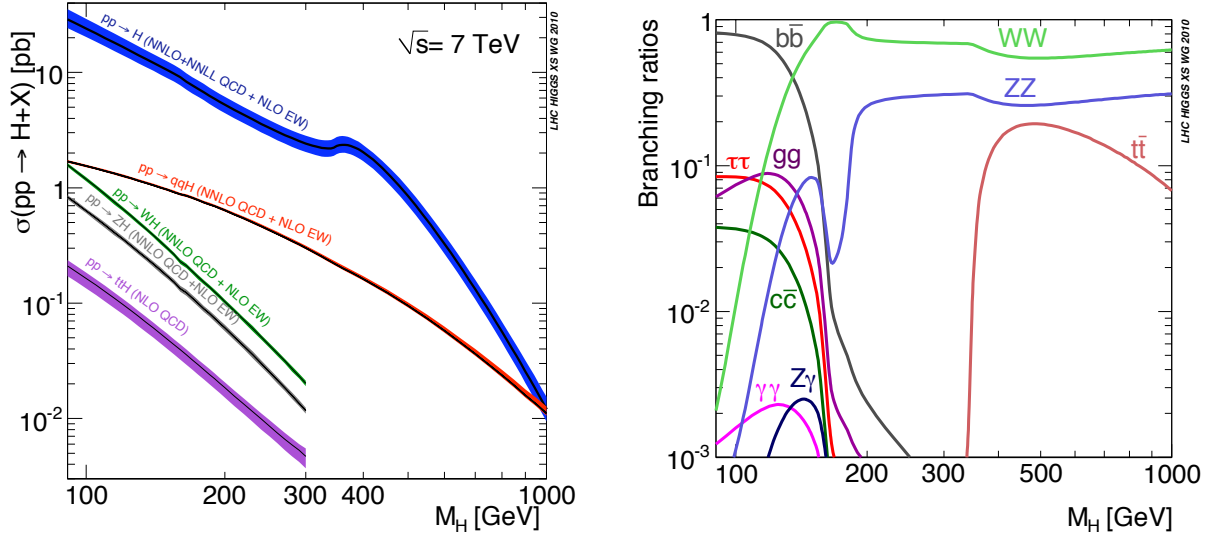
Figure 1: The standard model Higgs boson production cross sections (left) and decay branching fractions (right). The plots are taken from Ref. [9].
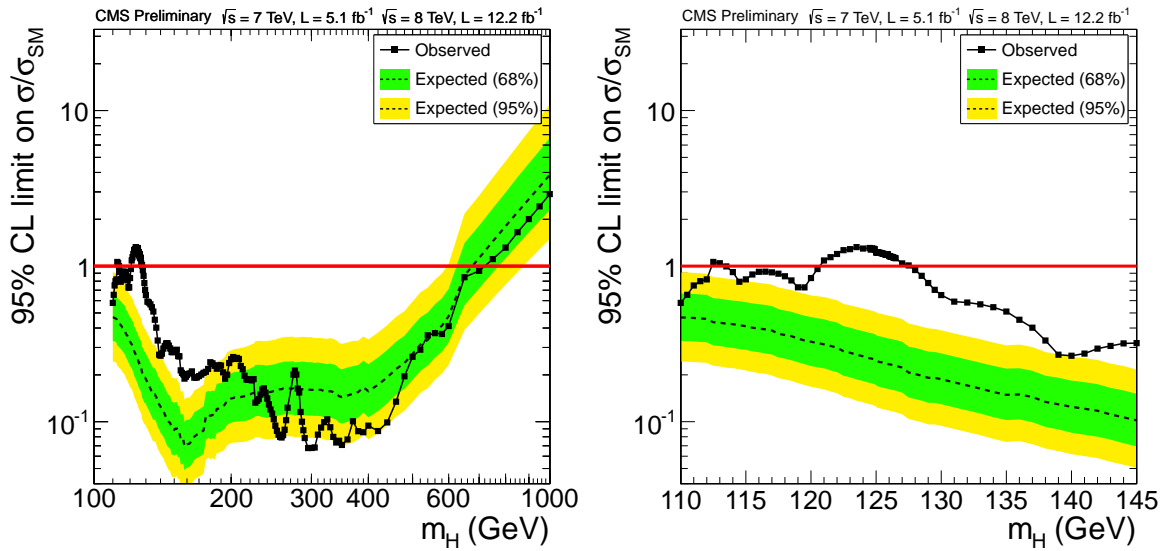

Figure 2: The observed and expected 95% CL upper limits on the signal strength parameter $\mu = \sigma/\sigma_{\rm SM}$ for the SM Higgs boson hypothesis as a function of the Higgs boson mass in the range 110–1000 GeV (left) and 110–145 GeV (right).
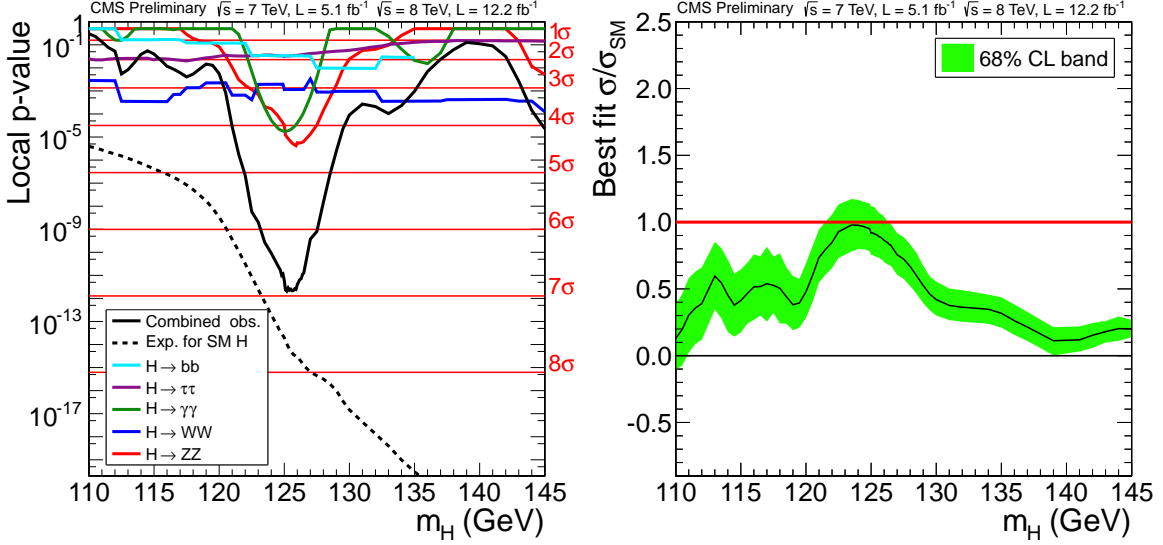
Figure 3: The observed local p-value p_0 (left) and best-fit $\hat{\mu} = \sigma/\sigma_{SM}$ (right) as a function of the SM Higgs boson mass in the range 110–145 GeV. The local p-values for individual channels and their combination are obtained with the asymptotic formula (lines); the combined local p-value is validated by generating ensembles of background-only pseudo-datasets (points). The dashed line shows the expected local p-values $p_0(m_H)$, should a Higgs boson with a mass mH exist. The band in the right plot corresponds to the $\pm 1\sigma$ uncertainties on the $\hat{\mu}$ values.
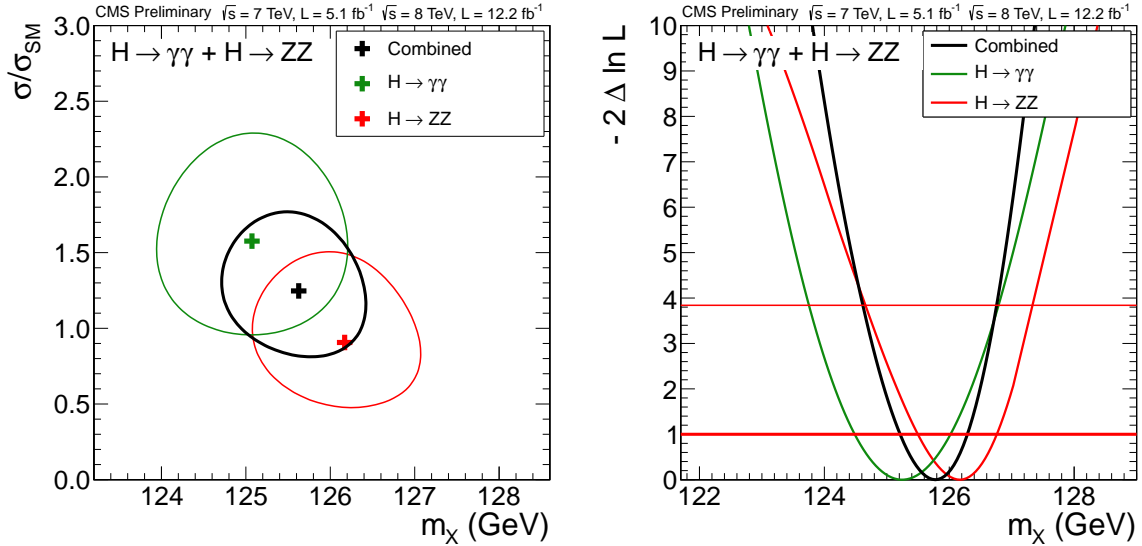

Figure 4: (Left) 2D 68% CL contours for a hypothesised boson mass m_X and signal strength $\mu = \sigma/\sigma_{SM}$ for the $\gamma\gamma$ and $4l$ final state, and their combination, assuming one common signal strength μ. (Right) 1D-scan of test statistic $q(m_X)$ (or -2 ΔlnL) vs hypothesised boson mass m_X for the $\gamma\gamma$ and $4l$ final states separately and for their combination. In this combination, three independent signal strengths $gg \to H \to \gamma\gamma$, $VBF + VH \to \gamma\gamma$, and $H \to ZZ \to 4l$ are profiled together with all other nuisance parameters.